Deuteron – α interaction by inversion of RGM S-matrix: determination of spin-orbit potential for spin-1 projectile

R. S. Mackintosh [1] and S.G. Cooper

Physics Department, The Open University,
Milton Keynes MK7 6AA

r.mackintosh@open.ac.uk, s.g.cooper@open.ac.uk

Abstract: The iterative-perturbative (IP) procedure for S-matrix to potential inversion is applied to spin-one projectiles for the restricted case of vector spin-orbit interaction only. In order to evaluate this extension of IP inversion we have inverted the multi-channel RGM S_{lj} of Kanada *et al* for deuterons scattering from ^{4}He with deuteron distortion and then compared the central components with those derived from RGM with spin set to zero. Attention is given to the question of how well the resulting potentials are established. Reliable spin-1 inversion is demonstrated. Results relating to inversion, to deuteron-nucleus interactions and to RGM are presented and suggest the range of nuclear interaction information which the procedure makes possible.

Keywords:
NUCLEAR REACTIONS Inverse scattering. Deuteron potentials. Resonating group.

PACS numbers: 21.45.+v, 24.10.-i, 25.10.+s, 25.45.-z, 25.60.Bx

February 9, 2008

[1]To whom correspondence should be addressed.

1 Introduction

For some time it has been straightforward to apply S-matrix to potential inversion to spin half projectiles, i.e., symbolically, perform the transformation $S_{lj} \rightarrow V(r) + \mathbf{l} \cdot \mathbf{s} V_{\rm so}(r)$. The same transformation for spin one particles is much more problematic, not least for the number of possible tensor forces, some of which couple certain projectile partial wave channels. Nevertheless, under certain circumstances, inversion for spin one projectiles should be possible, and one purpose of this paper is to present some specific cases in which previously published S_{lj} from RGM calculations of deuteron-^{4}He scattering are inverted. To assist in the evaluation of the resulting potentials, we also present potentials inverted from S_l from models which are similar except that the deuteron is treated as spinless.

Accordingly, we apply S-matrix-to-potential inversion to spin one projectiles for the restricted case where it is reasonable to assume that there is no tensor interaction. The S_{lj} are from multi-channel resonating group model (MCRGM) calculations. The algorithm which we employ is a natural extension of the IP method which has been successfully applied to spin-half S_{lj}, see Refs.[1, 2] and references therein. In Section 2 we explain the particular features of the source of S_{lj} which make an inversion involving only a vector spin-orbit interaction appropriate. In this paper we invert only S_{lj} which have been published elsewhere and we discuss only such aspects of the RGM calculations which are specifically relevant. An exhaustive account of what can be learned by applying inversion to RGM S-matrix requires RGM calculations of a complexity well beyond those leading to the S_{lj} which we invert. Nevertheless, the results presented here indicate what might be discovered from systematic studies linking inversion and RGM and similar theories. In another publication [3], deuteron-^{3}He potentials based on RGM are presented.

Inversion is not an end in itself and one of our goals is to establish generic properties of nucleus-nucleus potentials. It can also help to evaluate RGM and similar calculations, which, for all their complexity, are in general not yet capable of giving precise fits to experimental data. A particular strength of the RGM, of course, is that it contains an exact treatment of exchange terms and centre of mass motion. It is therefore not surprising that many of our findings relate to non-local effects and parity dependence, both of which have their origin in the exchange terms. In particular, we present evidence, based on an analysis of the imaginary components, for a form of non-locality very different from that which is dominant in nucleon scattering. This is in addition to the parity dependence which, as in other cases studied by inversion, turns out to be rather different from what has been assumed in phenomenological studies. The present inversions not only yield certain properties of deuteron-nucleus potentials, but suggest more general properties of nucleus-nucleus interactions.

Section 2 presents relevant details of the MCRGM calculations. Section 3 describes the generalisation of IP inversion to spin-1. Section 4 presents certain results for spin-0 deuteron inversions principally to help evaluate the spin-one inversions described in Section 5. Section 6 presents, for comparison with Section 5, potentials derived from earlier no-distortion spin 1 RGM. Section 7 summarises our conclusions concerning the inversion procedure itself and also presents certain findings about d-α potentials and discusses future work.

2 The Multi-channel RGM of Kanada *et al*

Kanada *et al* [4] (hereafter KKST) calculated d + α elastic scattering at several energies using multi-channel RGM (MCRGM) in order to study specific distortion effects. Spin-orbit but not tensor nucleon-nucleon forces were included and there was no coupling between $l = J - 1$ and $l = J + 1$ channels. For this reason, the calculated complex phase shifts were enumerated according to l and $J = l, l \pm 1$. The dynamic distortion of the deuteron was simulated by coupling to bound excited quasi-states of the deuteron. This coupling generates absorption, but insufficient absorption for the data to be fitted, ^{3}He + t channels being omitted for example. No D-state components were included in the deuteron and the coupling was exclusively to S-wave virtual states of the deuteron. In lowest order folding model, see Ref. [5] and references therein, it is the D-state which is responsible for the T_R [6] tensor term.[2]

The T_P tensor term is due to Pauli blocking [8], and this might be expected to be represented in fully antisymmetrized RGM. However since the T_P term depends on the suppression of effects due to the tensor component of the nucleon-nucleon interaction, see Ref.[8], the KKST S-matrix may not contain significant effects requiring a T_P interaction. The diagonal T_L interaction is expected to be small on general grounds [9].

The above features suggest that it is reasonable to represent the resulting S_{lj} with no more than a vector spin-orbit interaction added to the central potential.

KKST included an additional local and l-independent phenomenological imaginary potential in order to simulate the absorption from the excluded channels. Adjustment of the parameters of this imaginary potential led to acceptable fits to the angular distributions, but neither the tensor nor vector analysing powers were better than qualitative, the vector analysing powers being, unsurprisingly, more acceptable. The complex phase shifts were tabulated for CM energies of 8.0, 14.0, 19.6 and 37.33 MeV. In this paper we present and discuss potentials for the 19.6 and 37.33 MeV cases.

3 Inversion for spin-one projectiles

Inversion for spin-zero projectiles, involving the $S_l \rightarrow V(r)$ transformation, is now straightforward, and a variety of methods are available, see Refs. [10, 11]. Here we use the iterative perturbative, IP, method [1]; see Ref. [2] for recent developments.

The IP method allows inversion for spin-half particles, i.e. $S_{lj} \rightarrow V(r) + \mathbf{l} \cdot \sigma V_{\rm so}(r)$. Although the results are most naturally presented in terms of a central and spin-orbit component, one can think of this as equivalent to inverting the two sets of amplitudes for $j = l \pm 1$, leading to two corresponding potential components. The spin-one situation is much more complicated since there are three values of l for each j and, in general, coupling between $l = j - 1$ and $l = j + 1$ partial waves. The inversion of the full non-diagonal S-matrix to yield the general sum of vector and tensor components [6] is very challenging. Indeed, inversion from the incomplete and imprecise non-diagonal

[2]The full classification, based on symmetry principles, of the possible tensor forces was given by Satchler [6], who defined the three terms T_R, T_P and T_L. See also Robson [7].

S-matrix as generally determined empirically involves major ambiguity problems.

The calculations of KKST present the opportunity and motivation for a more restricted form of spin-one inversion. A straightforward extension of the IP method will be applied to the KKST S_{lj} yielding a potential of the form $V(r) + \mathbf{l} \cdot \mathbf{S} V_{\rm so}(r)$. Three sets of amplitudes determine two potential components, whereas for spin-half two sets of amplitudes determine only two potential components. It is not *a priori* obvious that this will be possible, at least yielding reasonably smooth potentials. Since T_R, T_P and T_L all have diagonal matrix elements, an arbitrary set of S_{lj} might contain effects which require representation by the diagonal parts of those components. In our restricted model, any effects which would be attributable in a full model to the diagonal tensor components will tend to induce 'waviness' in the potentials.

Since we must allow potentials fitting RGM S_{lj} to be parity dependent, there are twice as many components to be determined. The notation we have used previously [2] is that each real or imaginary, central or spin-orbit term has two components referred to as V_1 and V_2 components, defined as $V(r) = V_1(r) + (-1)^l V_2(r)$.

The combined effects of parity dependence, the limits on the numerical precision of the KKST S_{lj} and the uncertainty as to whether an $\mathbf{l} \cdot \mathbf{S}$ term is sufficient, are such that ambiguity problems could well be serious. An advantage of the IP procedure, compared to methods which simply take S_{lj}, 'turn a formal crank' and get $V(r)$, is that there is control over the ambiguities. It is actually quite important that *exact* inversion is avoided in cases where S_{lj} contain significant 'noise' due to numerical limitations (S_{lj} from theory) or fitting errors (empirical S_{lj}). Over-fitting is avoided by controlling the dimensionality of the inversion basis and adjusting the SVD singularity parameter (see Ref.[2] and references therein). Although the criterion for a 'smooth' potential is inevitably somewhat subjective, consistent results can be achieved. All the potentials presented below correspond to very low values of the convergence parameter σ defined [1] as

$$\sigma^2 = \Sigma_{lj} |S^t_{lj} - S^i_{lj}|^2 \tag{1}$$

where S^t_{lj} is the 'target' S-matrix for which we seek the potential, and S^i_{lj} is the S-matrix of the inversion potential. Unless we indicate otherwise, the potentials we present will be such that S^t and S^i would be indistinguishable on a graph, or very nearly so. Unfortunately, there can be a surprising range of potentials associated even with such low σ. This is true even with the extreme low σ (which we carefully avoid) associated with over-fitting numerical noise. We therefore study the uniqueness of inverted potentials by varying the 'starting potential' and the basis in which the final potential is expanded. Further substantiation comes from comparison with d-α potentials derived from RGM calculations in which spin degrees of freedom are omitted.

4 Conclusions from spin-zero deuteron models

Uncertainties connected with the omission of tensor forces suggest that, in attempting to establish spin-one deuteron-nucleus potentials, we should compare the spin-independent parts of the potentials with potentials found in studies where the complication of spin is avoided. We therefore describe some results from calculations involving

S-matrices from RGM calculations in which the deuteron is treated as spinless. We find, *inter alia*, (i) that we must not omit parity dependent components of the potential, and, (ii) that the exchange kernel will have an effect on the imaginary potential unlike that for nucleon scattering.

4.1 Real potential, spin-zero case

We inverted phase shifts [12] for 20, 40, 60 and 80 MeV CM d + Alpha RGM calculations in which Coulomb and spin-orbit terms were omitted. There was no channel coupling and no phenomenological representation of absorption, so the resulting potentials were real. For each energy, we had real phase shifts for $0 \leq l \leq 8$ so that at the two highest energies, the phase shifts for the highest available partial waves were far from zero. For this reason, there is no meaning attributable to $V(r)$ for $r > R(E)$, where $R(E)$ is the upper radius over which the inversion basis was defined at energy E; $R(20) = R(40) = 8$ fm, $R(60) = 7$ fm and $R(80) = 6$ fm. These values were found empirically by requiring that smooth potentials should exist.

The relevant finding is that when all the exchange terms, explicitly including the '2-exchange' [13] terms, are included in the RGM calculation, the local equivalent potential is substantially parity dependent. Although the parity dependent component falls with energy, it is appreciable at 80 MeV CM. We therefore expect such terms in the lower energy spin-dependent cases discussed below. The parity dependent potential V_2 does not follow the form of the parity independent term, but is surface peaked. It is such that the the *even* potential is deeper, notably for 2—5 fm. For 20 MeV deuterons, V_2 is attractive so that at 4 fm, where $V_1 \sim 5$ MeV, the ratio of even to odd potential is about 2:1. The effect falls with energy but the qualitative pattern is retained. At 60 MeV the V_2 term is largest around 2.5 fm at which radius the even parity potential is some 2.5 MeV deeper than the odd parity potential. We conclude that when spin is included, we must allow all components of the potential to be parity dependent.

The same S-matrix elements can also be subjected to energy dependent inversion [2] in which the potential is expressed as a product of energy function and a fixed radial form. The present data are well represented by

$$(1 - 0.00237E)V_1(r) + (-1)^l(1 - 0.00919E)V_2(r) \tag{2}$$

where $V_2(r)$ is a surface peaked attractive term with a maximum magnitude at $r = 3$ fm where its value is -2.2 MeV. The qualitative features of the potential are just those found with fixed energy inversion apart from the change in radial form with energy. Equation 2 implies that the parity dependent term becomes zero around 109 MeV, so we must presume parity dependence for both energies in the spin-1 inversions.

4.2 Complex deuteron potential at 55 MeV

Thompson and Tang [14] calculated d + α elastic scattering at 55 MeV CM using no-distortion RGM with a local l-independent phenomenological imaginary potential to simulate absorption. They adjusted the parameters of the imaginary potential to

achieve a reasonable fit to the elastic scattering differential cross section. No spin effects were included.

The tabulated S_l of Thompson and Tang were inverted and the salient features of the resulting potentials were as follows:

1. Smooth potentials closely reproducing S_l could be found if and only if the potential had a substantial parity dependent (V_2) component. The properties of the parity dependent potential were well-determined.

2. In the outer radial region, $r \geq 2.5$ fm, the imaginary V_1 potential follows quite closely the local imaginary potential ('bare' potential) incorporated in the RGM. However, towards the nuclear centre, particularly for $r \leq 1.5$ fm, it is much *deeper* than the bare potential.

3. The real V_2 term is purely attractive, has a maximum magnitude of 2.5 MeV at about 1.8 fm and is near zero at the origin. It is therefore in essential respects the same as in the real potential case in Section 4.1.

4. The imaginary V_2 term is repulsive, peaking near 1.5 fm with a maximum of about 1 MeV.

5. The volume integral of the real V_1 component is well determined by inversion and is reasonable at 470 MeV fm^3 per projectile nucleon at a laboratory energy of 82.5 MeV (41.25 MeV per projectile nucleon.)

If there were no exchange terms and the consequent non-locality, the inversion should yield an imaginary component precisely equal to the added phenomenological imaginary potential. But this is not found, the imaginary potential being substantially *enhanced* at the nuclear centre. Remarkably, the effect of Perey-type non-locality is the reverse [15]: this is an 'anti-Perey effect'. This is a firm conclusion; for example, the form of the imaginary V_1 component is essentially the same even when the parity dependent (V_2) components are excluded. (Such inversions lead to much larger values of σ but yield V_1 components with similar properties.) It seems that the form of non-locality responsible for this effect is independent of the exchange processes which lead to V_2 (parity dependence) terms. The 'Perey-like' effects which arise in the presence of single nucleon 'knock-on' exchange are discussed, for example in Ref [15]. In the presence of a Perey-Buck non-local potential [16] which simulates very well the knock-on exchange seen by single nucleons [15], one finds that inversion leads to a uniformly *reduced* imaginary potential, very satisfyingly consistent with what one would expect on the basis of a conventional Perey [17] effect. The existence of the reverse effect in RGM calculations of the scattering of $A \geq 2$ projectiles is therefore striking evidence for the very different action of other [13] exchange terms in the kernel.

The character of the V_2 term is consistent with the results of Section 4.1: V_2 is essentially surface peaked corresponding to additional attraction for the even parity partial waves. Its maximum value, about 2.5 MeV, is consistent with the 60 MeV case of the last section, but the maximum is at about 1.7 fm, whereas the radius of the maximum was about 2.5 fm for the 60 MeV case.

5 Inversion of KKST complex phase shifts

We present results for the 37.33 MeV case before those for the 19.6 MeV case. At the lower energy there is considerably less information to determine the potential and it is appropriate to exploit information from the higher energy case. At 37.33 MeV, S_{lj} were calculated for $l \leq 10$ but at 19.6 MeV, only for $l \leq 8$.

The behaviour of $|S|$ in Figure 6 of KKST suggests a much greater imaginary potential at the higher energy, a natural consequence of the larger number of open channels. It also suggests a substantial imaginary spin-orbit component at both energies since $|S_{lj}|$ is much smaller for $j = l + 1$ than for $j = l - 1$. The difference is too great to be a second order consequence of the real spin-orbit potential.

5.1 Deuteron-α interaction at 37.33 MeV CM

For each $l > 0$, there are 3 complex phase shifts. Hence, with $l \leq 10$, the IP procedure can handle up to 62 real basis functions before the linear system becomes under-determined. This means that of the four complex components, central and spin-orbit terms, each with parity independent and parity dependent components, three can have bases of dimensionality 8 and one of 7. Since there are phase shifts for three j values for each l, we might not be surprised to find that spin-orbit components required bases of the higher dimensionality (and so it turned out). For most of the calculations we used a harmonic oscillator basis [18] with $R_0 = 1.48$ and we assumed the potential was zero beyond $R_{\max} = 7.5$ fm. Even with 31 basis functions for both real and imaginary components we could not achieve the 'perfect fit' low σ values achieved for the zero spin 55 MeV case, so the final potentials are less unique.

A potential, 'pot3', was found for which the larger components were free of waviness and for which $\sigma = 0.00173$. There was no discernible difference between S^t and S^i when plotted. Alternative potentials were found when using different starting potentials or different bases, but potentials for which σ was lower looked like pot3 but with superimposed waviness due to over-fitting. Figure 1 presents the complex central and spin-orbit V_1 components together with those for 19.6 MeV discussed below, and Figure 2 presents the corresponding V_2 (parity dependent) components. Table 1 presents volume integrals and RMS radii for the real central V_1 parts of 'pot3' and also of a somewhat more oscillatory potential, 'pot1'. Potential pot1 gave a poorer fit to S_{lj} than pot3 as can be seen from σ. Most components of pot1 exhibited typical over-fitting oscillations about the pot3 forms, yet the volume integrals and RMS radii were almost the same.[3] The volume integrals of the larger components of pot3 are consistent with global optical potentials. We note the following features of pot3:

1. The imaginary V_1 potential follows the phenomenological imaginary potential (not shown in Figure 1) quite closely for $r \geq 2.5$ fm. However, towards the

[3]The somewhat paradoxical situation where pot1 shows some waviness indicative of over-fitting yet gives worse σ than pot3 is due to the fact that certain small components were different in form, and the oscillations in the larger components were induced by the iterative procedure trying to lower σ with apparently incorrect solutions for the smaller components.

nuclear centre, particularly for $r \leq 1.5$ fm, it becomes very much *deeper* than the bare potential to a much greater degree than for the 55 MeV case. This is not solely an effect of the non-locality as it was for 55 MeV since the multi-channel RGM itself does contribute via deuteron breakup. Remarkably, the open channels make virtually no contribution to the imaginary V_1 for $r \geq 2.5$ fm, something also found [3] in the d $+^3$He case. The absorptive potential induced by these coupled channels has a very deep minimum, about 25 MeV deep, at the nuclear centre. The non-zero slope of V_1 at $r = 0$ indicates that it is a local representation of a non-local or l-dependent potential. (In this context, by l-dependence we mean variation across l-values of particular parity, certainly possible for potentials generated by inelastic processes.)

2. The real V_2 term is mostly attractive with a local a maximum magnitude of 2 MeV near 2.7 fm. It approaches zero at 1.8 fm and is quite large near the origin. This is very similar to the 55 MeV V_2 term and consistent with the cases mentioned in Section 4.1.

3. The imaginary V_2 term is absorptive. It is not much like the corresponding 55 MeV term, but this might be due to the fact that here the multi-channel RGM itself gives rise to absorption. The V_2 term is almost a third of the magnitude of V_1 term near 2.5 fm, the radius at which the bare potential peaks and where, see point 1, V_1 hardly differs from the bare potential.

4. The volume integral per target nucleon of the real V_1 component, $J_{\rm R}$, is well determined at about 480 MeV fm^3 per projectile nucleon. This is phenomenologically reasonable for a laboratory energy of 56 MeV (28 MeV per projectile nucleon.)

5. The imaginary spin-orbit terms are quite small but not zero. The parity dependent terms are generally small except near the origin.

6. Although the real spin-orbit term is smooth, it is not known why it should be peaked at the nuclear centre rather than being of Thomas form. Possibly it is simulating a T_L term.

How well-established are these properties? In order to study the uniqueness of the potential, we performed inversions with an alternative inversion basis (Gaussians) and with alternative starting potentials. In Figures 3 and 4, we compare pot3 with potentials 'potG1', the lowest-σ solution found using a Gaussian basis that was not conspicuously wavy. The characteristics of the central V_1 components of potential potG1 are included in Table 1, with $J_{\rm R}$, r-RMS and $J_{\rm I}$ being essentially the same as for pot3. The larger-magnitude components visible in Figures 3 and 4 show that 'potG1' is essentially pot3 with superimposed waviness, so that in view of the substantially larger σ, the comment in the footnote 3 applies. Since we find quite small imaginary spin-orbit components, we inverted with imaginary spin-orbit terms held zero, and found that such terms were essential, even though they are small and less well-determined than other terms. We conclude that pot3 is a reliable representation of the local potential corresponding to the 37.33 MeV KKST S_{lj}.

In Table 1 we include for comparison the phenomenological optical potential of Hintenberger *et al* [19] for deuterons scattering from ^{4}He at 52 MeV laboratory energy.

Table 1: Properties of central potentials (V_1 terms) for 37.33 MeV and 19.6 MeV deuterons, KKST S-matrix.. OM refers to the optical model of Hintenberger*et al*

Solution	σ	$J_{\rm R}$	r-RMS (real)	$J_{\rm I}$	r-RMS (imag)
37.33 MeV					
pot1	0.00320	478.15	2.960	136.22	3.487
pot3	0.00173	479.86	2.962	136.85	3.463
potG1	0.00486	483.33	2.961	137.56	3.429
OM	—	539.48	2.68	170.66	3.211
19.6 MeV					
pot-a	0.903×10^{-3}	499.72	2.905	101.75	3.448

5.2 Deuteron-α interaction a 19.6 MeV CM

As noted above, there are fewer S_{lj} to fix the same number of potential components. The 37.33 MeV potentials were used as starting potentials. Figures 1 and 2 show components of 'pot-a' which reproduces the 19.6 MeV KKST S_{lj} with $\sigma = 0.000903$. Characteristics of pot-a are given in Table 1. We find:

1. The real, central V_1 component is smooth and substantially deeper at the nuclear centre than for 37.33 MeV. This reasonable depth dependence is largely due to exchange since the nucleon-nucleon interaction is fixed. The volume integral is correspondingly larger than for 37.33 MeV.

2. A remarkable difference is the complete absence of one of the most striking features in the 37.33 MeV case: the deep central dip in the imaginary central V_1 component. There is a corresponding 30% decrease in the volume integral. We attempted unsuccessfully to find potentials which did not have this property.

3. The real central V_2 term is more attractive than for 37.33 MeV except for $r < 1$ fm. This is consistent with the trend found in Section 4.1 that V_2 is attractive and increases with decreasing energy.

4. All the other imaginary components are substantially different at the two energies.

5. The real spin-orbit components, both V_1 and V_2, are remarkably similar at the two energies.

Concerning point 2: The difference between the 19.6 MeV and 37.33 MeV potentials is not surprising in view of the considerable difference, clearly evident in KKST, between $|S_{lj}|$ for 19.6 and 37.33 MeV, including the large spread of values for different j for given l. There is much to be learned as to how the imaginary potential develops with energy as channels open and this question bears upon our general understanding of how inelastic processes give rise to absorption.

Just as for 37.33 MeV, various tests were performed to verify that the potential is reliably determined. We established, too, that an imaginary spin-orbit potential is

required, though the relative accuracy of this small term is less than for the other components.

6 S-matrix of Lemere, Tang and Thompson

The earlier study of d + α scattering by Lemere *et al* [23] omits all deuteron excitation but does include spin-orbit terms in the NN interaction and, moreover, covers a considerable energy range. Although a somewhat different NN interaction was used, it presents an opportunity to disentangle deuteron distortion and spin-orbit effects. We determined potentials corresponding to their RGM S_{lj} for CM energies of 16.58 MeV, 24.87 MeV and 53.9 MeV (i.e. up to 80.85 MeV laboratory energy.) Absorption was represented solely by a local imaginary potential[4]. For 53.9 MeV, only J-averaged phases were provided for the highest l-values, i.e. $l = 9$, 10, and 11.

As with other spin-1 inversions, ambiguities arise, particularly if the restriction to reasonably smooth potentials is abandoned in pursuit of very low σ. Again, this is probably due to the inadequacy of the $\mathbf{L} \cdot \mathbf{S}$ form fully to represent the lj dependence implicit in the S_{lj}. In order to establish reliable potentials, we applied alternative basis sets etc. to the 24.87 MeV S_{lj}. The optimum solution at 24.87 MeV served as a starting potential at 16.58 and 53.9 MeV. We considered it important to achieve a uniform set of potentials for the three energies, with at least the largest component (the real, central V_1 term) changing in a regular fashion over the energy range, and only the smallest components (such as the imaginary V_2 spin-orbit term) varying greatly from case to case. This makes it possible to attribute physical meaning to the energy dependence of the large components.

The optimum potentials are presented in Figures 5 and 6. Volume integrals and rms radii of the real central V_1 term are presented in Table 2 with corresponding values of σ. Two alternative solutions for 16.58 MeV are presented, giving some idea of how well determined the potential is. The larger σ at 53.9 MeV is significant; much lower values corresponding to very wavy potentials were rejected. In part, the larger σ reflects the larger number of terms in the sum in Equation 1. Possibly, the inadequacy of the simple spin-orbit form is greatest at the highest energy, evidence for this being that, although the value of σ given for 53.9 MeV in Table 2 corresponds to a visually perfect fit to S_{lj}, the discrepancy in the observables is noticeable, particularly in the tensor analysing powers. We may also be seeing a consequence of the j-averaged S_{lj} for $l \geq 9$. At 16.58 and 24.87 MeV, the inversion potentials give phase shifts yielding observables which are graphically indistinguishable from those calculated directly from the RGM S_{lj}.

Despite the higher σ at 53.9 MeV, regular behaviour is apparent. However, the nature of the energy dependence is unexpected. We see from Figure 5 that the depth of the real, central V_1 component at the nuclear centre falls steadily with energy as did the same term in Figure 1. But there is no corresponding fall in the volume integral J_{R} in Table 2. Figure 5 shows this component systematically *increasing* with energy in the

[4]For other details see Lemere *et al*; we are grateful to Professor Tang for bringing this to our notice and suggesting the present calculations.

Table 2: Characteristics of real central V_1 potential reproducing S_{lj} of Lemere *et al.*

CM energy	σ	J_{R}	r-RMS (real)
16.58	0.00314	543	3.079
16.58	0.00136	552	3.070
24.87	0.00767	552	3.111
53.9	0.0173	557	3.137

surface region, a phenomenon reflected in the steady increase in rms radius, Table 2. The physical reason for this may well be an effect of two-nucleon exchange processes, an effect which seems to have been compensated for in the calculations of the previous section by increasing surface repulsion due to deuteron distortion. The fall with energy of the potential at the nuclear centre is what would be expected from single nucleon knock-on exchange (in the absence of channel coupling, the energy dependence of the real potential is entirely due to exchange.) Although the NN interaction of Lemere *et al* differs somewhat from that of KKST, the difference is unlikely to account for the different surface behaviour of the real potential.

A further clue to the nature of the exchange processes lies in the imaginary central V_1 potentials. In the RGM calculations of Lemere *et al*, the absorption is entirely due to an added local imaginary potential. If the non-local kernels were omitted from the RGM, the inversion would, of course, reproduce the local kernel and the added local imaginary potential terms (with zero V_2 terms). The very different imaginary V_1 potentials displayed in Figure 5 are a consequence of the fact that the local imaginary potential is 'seen' by a wave-function which is itself largely determined by a non-local effective potential.Such behaviour was found already in section 4.2 where we discussed 'anti-Perey' behaviour in the 55 MeV spinless case. The behaviour shown in Figure 5 is also 'anti-Perey' at the nuclear centre to an extent which increases with energy. Comparing the imaginary central V_1 potentials with the imaginary potentials included in Ref [23] reveals a Perey-like reduction in the surface region, but an enhancement at the nuclear centre. This occurs at each energy, and varies systematically, with the smallest surface reduction and central enhancement at the lower energies, and a large (Perey-like) surface reduction but small enhancement for $r \leq 1.5$ fm at 53.9 MeV. Referring back to Figure 1, we see that there is a similar strong anti-Perey effect at 37.3 MeV but not at 19.6 MeV. Clearly, apart from generating V_2 potentials, those exchange terms which are not of the one-nucleon (knock on) exchange type also have a substantial effect on the interaction of deuterons with nuclei.

One of the most surprising features which was found for KKST potentials at both energies, the deep real V_1 spin orbit potential, occurs consistently in Figure 5.

In summary, certain striking features of the KKST potentials recur for the case without deuteron distortion, but there certain differences which suggest that a systematic study involving extended RGM calculations will yield much interesting insight into the combined influence of antisymmetrization and channel coupling to inter-nuclear interactions.

7 Discussion, conclusions and future work

Conclusions relating to inversion. The inherent flexibility of the IP algorithm has allowed us to perform inversion for spin-one projectiles where there is no coupling between l channels for given j and we can justify the omission of a tensor interaction. We can incorporate *a priori* information, allowing us to invert when the amount of information to fix each potential component is quite low (e.g. the use of the 37.33 MeV solution in the 19.6 MeV case).

The potentials. We have determined potentials representing the KKST S_{lj} for 37.33 and 19.6 MeV. The real components are remarkably similar apart from the expected energy dependence. General features are consistent with those derived from a spinless model, and there is every reason to believe the potentials are reliable.

It is interesting therefore that the various imaginary components at the different energies differ quite markedly, particularly for $r < 1$. Although the potential components are least reliably determined for $r < 1$ fm, and do possibly interact with each other in the inversion process, it is a firm conclusion that the imaginary potential is of very different form at 19.6 and 37.3 MeV. This includes notably the large magnitude of the central V_1 term at smaller r. The larger number of open channels at the higher energies makes such a difference in imaginary potential plausible. However the form of the imaginary potential must certainly be influenced by the fact that only $\Delta l = 0$ transfer was included in the KKST calculations. CDCC calculations [20] at higher energies suggest [21] that breakup into $l = 2$ states of the deuteron modifies the absorptive potentials at larger radii.

In view of the uncertainty associated with fitting S_{lj} for spin-one projectiles with a vector spin-orbit potential alone, it is interesting that a universal property of the real spin-orbit V_1 term has emerged. This term is, in every case, whether there is deuteron distortion or not, essentially the same: i.e. a surprisingly deep potential hole at $r = 0$. The corresponding V_2 term nearly always shares this property. The interpretation of this requires further study; perhaps it is the consequence of representing with a vector potential that which would be better represented by a tensor potential. The fact that in the present case S_{lj} can indeed be represented by a vector term alone points to the ambiguity problems which lie ahead for studies involving tensor potentials.

Conclusions relating to RGM and MCRGM. The results here are no more than a first step in extracting information concerning the deuteron-nucleus potential from RGM calculations. The possibilities for studying the way different NN potentials or different reaction channels included in the RGM model manifest themselves in the single particle local potential are obvious. The model of KKST leads to a potential with certain broad features corresponding to the phenomenological Woods-Saxon based OM, but having differences in detail. In particular, the RMS radius of the real component is larger than the OM value, although not too much weight should be given to Woods-Saxon phenomenology with mediocre fits. It is satisfying that the volume integral of the KKST imaginary central potential rises with increasing energy as the volume integral of the real part falls. It is also appropriate that the latter falls rather more slowly than that for the nucleon potential. The contrary behaviour *in the surface, only*, of the potential derived from Lemere *et al* S_{lj} is one of many observations deserving

systematic study. The need for MCRGM calculations which include higher l-transfer to $l > 0$ deuteron virtual states is a high priority if it is true that the CDCC findings apply in general.

Conclusions relating to deuteron-nucleus interactions. Caution is needed in extrapolating from the deuteron-α interaction to general properties of deuteron-nucleus potentials. Indeed, the magnitude of the parity dependent components will fall with increasing A of the target nucleus. Nevertheless, the present study does suggest that deuteron-nucleus potentials have certain features which are not generally allowed for in phenomenological studies. One such feature is the very deep dip near $r = 0$ in the imaginary potential, possibly related to unusual non-local or l-dependence effects. The lowest order deuteron folding model implies [22] that the non-locality range of the deuteron-nucleus potential is half that of the folded-in nucleon-nucleus non-locality. But the present work shows that a fully antisymmetrized system with channel coupling involves other forms of non-locality as well. The 'anti-Perey' effect, possibly due to two-nucleon exchange terms in the kernel, is evidence for this.

General conclusions concerning inter-nucleus potentials. The results presented here suggest generic properties which are almost never represented in conventional phenomenology based on Woods-Saxon potentials. While some of these properties will certainly be attenuated for heavier target nuclei, they show that conventional phenomenology does not provide a sound basis for the comparative evaluation of relativistic and non-relativistic approaches.

Future RGM calculations. A systematic RGM study combined with inversion could clearly yield much information concerning both RGM and inter-nuclear interactions. Some steps in this direction are underway [3], but the questions raised by the present work require very substantial RGM calculations indeed. In the first place, the clear indication of CDCC calculations that the $l = 2$ states of the virtual deuteron are important imply that these should also be included in RGM. Moreover, CRC calculations of deuteron scattering on heavier nuclei [24] suggest that coupling to mass the three reaction channels play an important role. This unexpected result requires confirmation in a fully antisymmetrized RGM calculation in which the various doubts concerning non-orthogonal channels which plague CRC calculations do not enter. Finally, there remains the challenge of studying the consequences of using more realistic potentials (tensor interaction, repulsive cores, etc.), see for example Ref. [25].

Acknowledgements

We are most grateful Professor Y. C. Tang for tabulated phase shifts and helpful advice and to the Engineering and Physical Science Research Council of the UK for grants.

References

[1] S.G. Cooper and R.S. Mackintosh, Inverse Problems, **5** (1989) 707

[2] S.G. Cooper and R.S. Mackintosh, Phys. Rev. **C54** (1996) 3133

[3] S.G. Cooper, 'Antisymmetrization and channel coupling effects on the imaginary potentials for p $+\alpha$/d $+^3$He' OU preprint OUPD-9707

[4] H. Kanada, T. Kaneko, S.Saito and Y.C. Tang, Nucl. Phys. **A444** (1985) 209

[5] P.W. Keating and D.D. Armstrong, Phys. Rev. **C8** (1973) 1692

[6] G.R. Satchler, Nucl. Phys. **21** (1960) 116

[7] B.A. Robson, The Theory of Polarization Phenomena, (Clarendon Press, Oxford, 1974)

[8] A.A. Ioannides and R.C. Johnson, Phys. Rev. **C17** (1978) 1331

[9] A.P. Stamp, Nucl. Phys **A159** (1970) 399

[10] K. Chadan and P.C. Sabatier, Inverse Problems in Quantum Scattering Theory, Second Edition, (Springer, New York, 1989)

[11] R.S. Mackintosh and S.G. Cooper, Invited Contrib. to Int. Symp. on Quantum Inversion Theory and Applications, Bad Honnef *Springer Verlag, Berlin, 1994*

[12] Y. C. Tang, private communication.

[13] M. LeMere, D.J. Studeba, H. Horiuchi and Y.C. Tang, Nucl. Phys. **A320** (1979) 449

[14] D.R. Thompson and Y.C. Tang, Phys. Rev. **C8** (1973) 1649

[15] R.S. Mackintosh and S.G. Cooper J. Phys. G. **23** (1997) 565

[16] F. Perey and B. Buck, Nucl. Phys. **32** (1962) 353

[17] F.G. Perey, in: Direct interactions and nuclear reaction mechanisms, eds. E. Clementel and C. Villi (Gordon and Breach, New York, 1963); N. Austern, Phys. Rev. **B137** (1965) 752

[18] V.I. Kukulin, private communication.

[19] F. Hintenberger, G. Mairle, U. Schmidt-Rohr, G.J. Wagner and P. Tureck, Nucl. Phys. **A111** (1968) 265

[20] M. Yahiro, M. Nakano, Y.Ieri and M. Kamimura, Prog. Theor. Phys. **67** (1982) 1038; H. Amakawa, A. Mori, H. Nishioka, K. Yazaki and S. Yamaji, Phys. Rev. **C 23** (1981) 583; I.J. Thompson and M. Nagarajan, Phys. Lett. **106B** (1981) 163

[21] A.A. Ioannides and R.S. Mackintosh, Phys. Lett. **169B** (1986) 113

[22] P.D. Kunz, Phys. Lett. **35B** (1971) 16

[23] M. Lemere, Y.C. Tang and D.R. Thompson, Nuclear Physics **A266** (1976) 1

[24] R.S. Mackintosh, S.G. Cooper and A.A. Ioannides, Nucl. Phys. **A472** (1987) 85

[25] H.M. Hofmann and G.M.Hale, Nucl. Phys. **A617** (1997) 69

Figure Captions

Figure 1. Potentials found by inverting KKST S_{lj} for deuterons scattering from ^{4}He. The dashed line represents the pot3 solution for 37.33 MeV CM, and the solid line solution pot-a for 19.6 MeV. These are the V_1, i.e. parity independent components arranged in order from from the top: real central, imaginary central, real spin-orbit and imaginary spin-orbit.

Figure 2. The parity dependent, V_2, components for the same cases as shown in Figure 1.

Figure 3. Comparison of V_1 components for the pot3 (solid lines) and potG1 (dashed lines) solutions for 37.33 MeV deuterons.

Figure 4. Comparison of V_2 components for the pot3 (solid lines) and potG1 (dashed lines) solutions for 37.33 MeV deuterons.

Figure 5. The parity independent, V_1, components for 17 MeV (solid), 25 MeV (dashed) and 54 MeV (dotted) deuterons scattering from ^{4}He, derived by inverting the S_{lj} of Lemere *et al.*

Figure 6. As for Figure 5, but here the V_2 components are plotted.

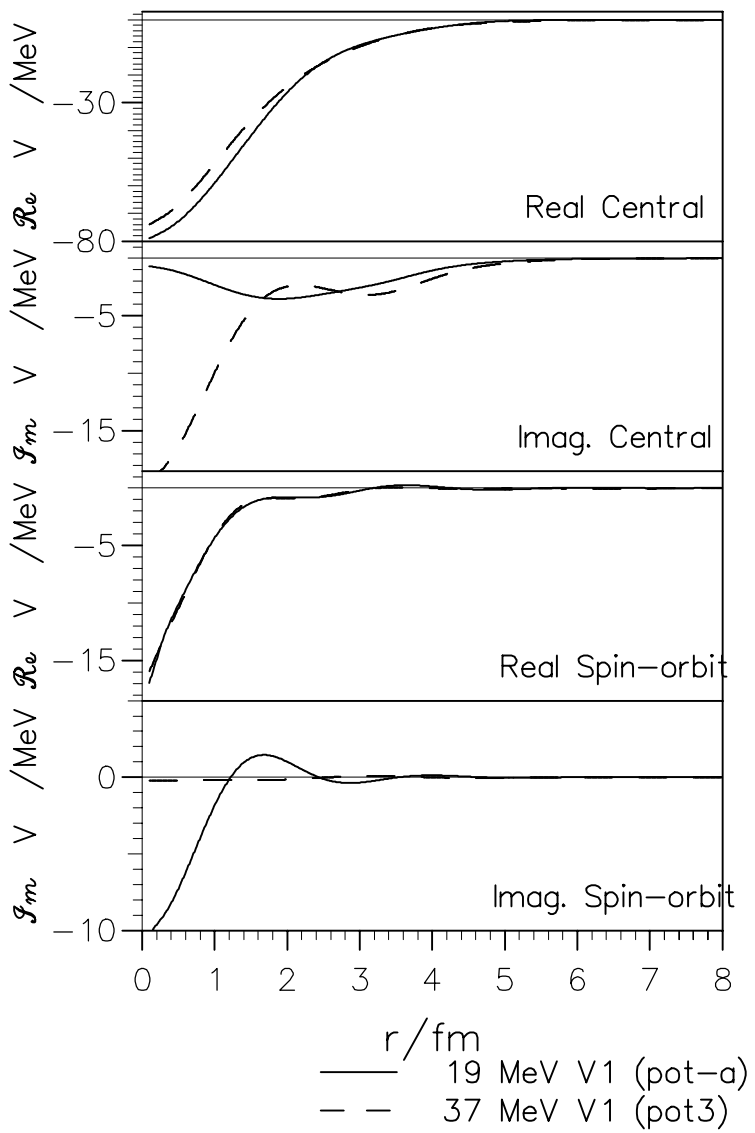
Real Central
Imag. Central
Real Spin–orbit
Imag. Spin–orbit
−30
−80
−5
−15
−5
−15
0
−10
0 1 2 3 4 5 6 7 8
r/fm
19 MeV V1 (pot–a)
37 MeV V1 (pot3)

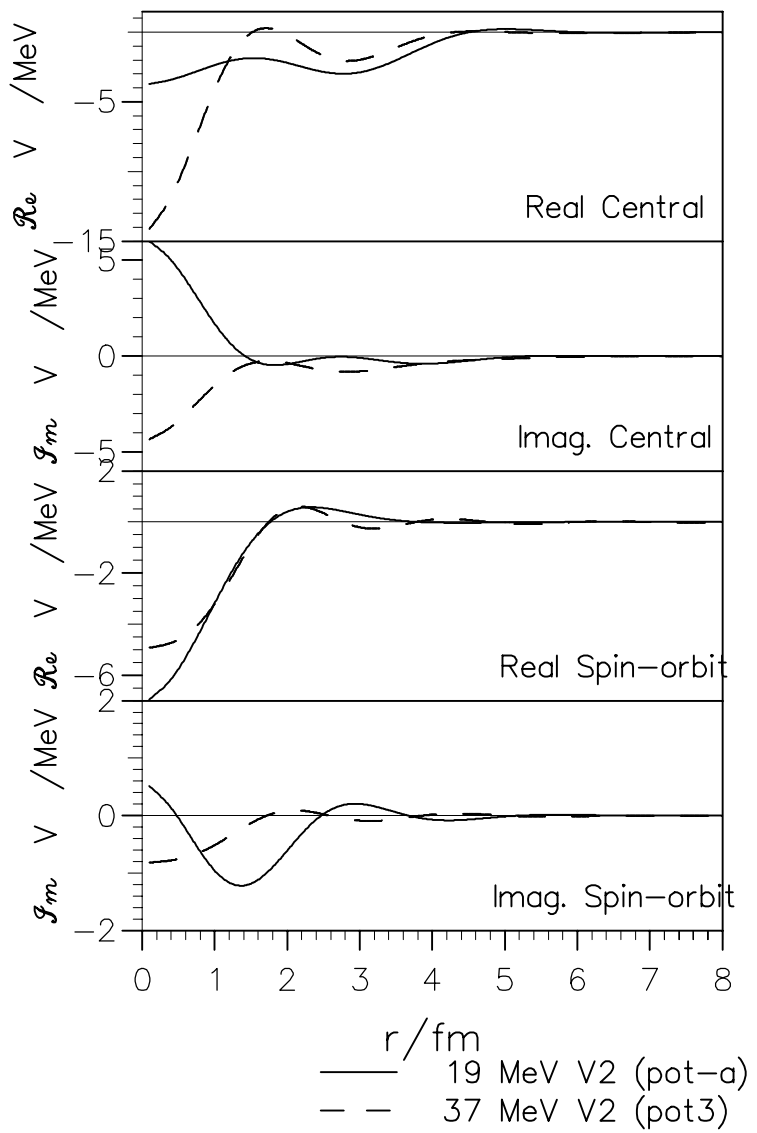
Re V /MeV
−5
Real Central
15
5
0
−5
Im V /MeV
Imag. Central
2
−2
−6
Re V /MeV
Real Spin−orbit
2
0
−2
Im V /MeV
Imag. Spin−orbit
0 1 2 3 4 5 6 7 8
r/fm
19 MeV V2 (pot−a)
37 MeV V2 (pot3)

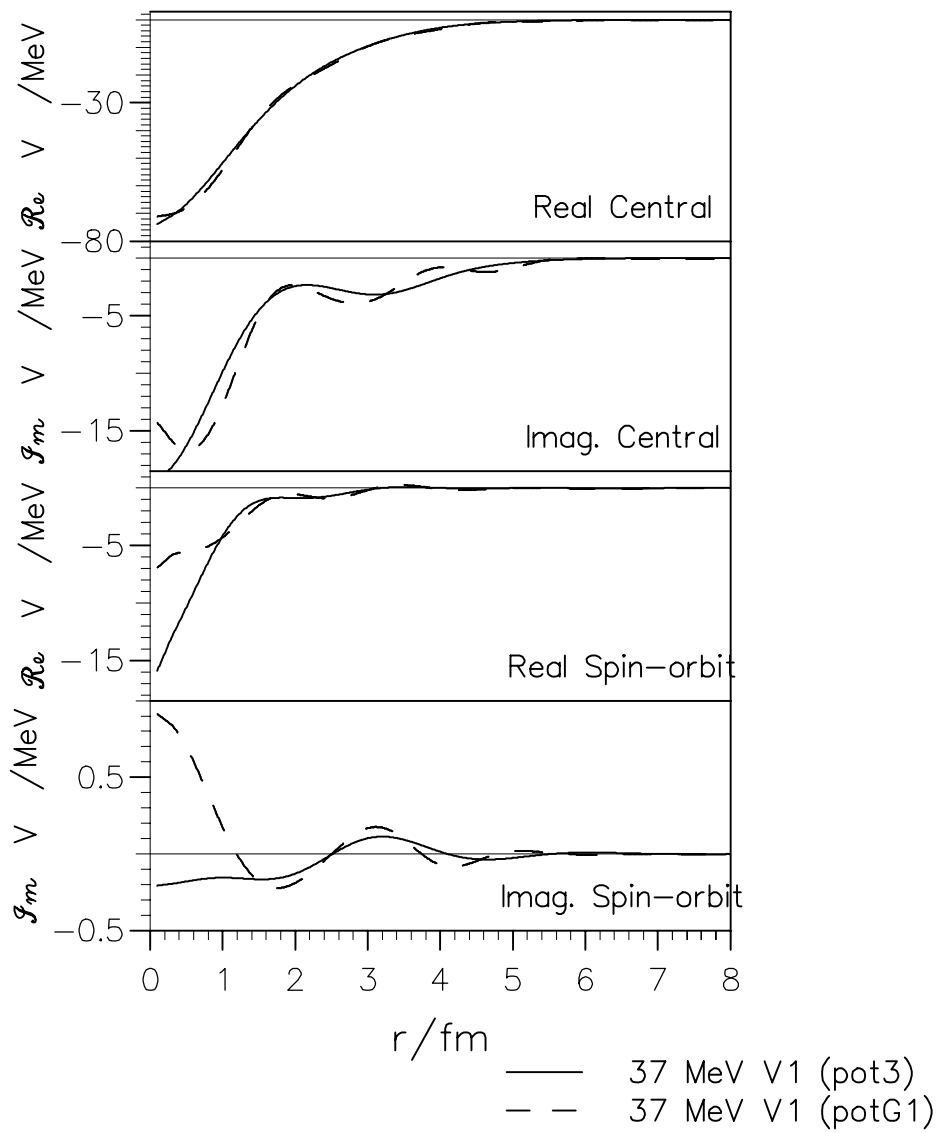
Real Central
Imag. Central
Real Spin–orbit
Imag. Spin–orbit
−30
−80
−5
−15
−5
−15
0.5
−0.5
0
1
2
3
4
5
6
7
8
r/fm
37 MeV V1 (pot3)
37 MeV V1 (potG1)

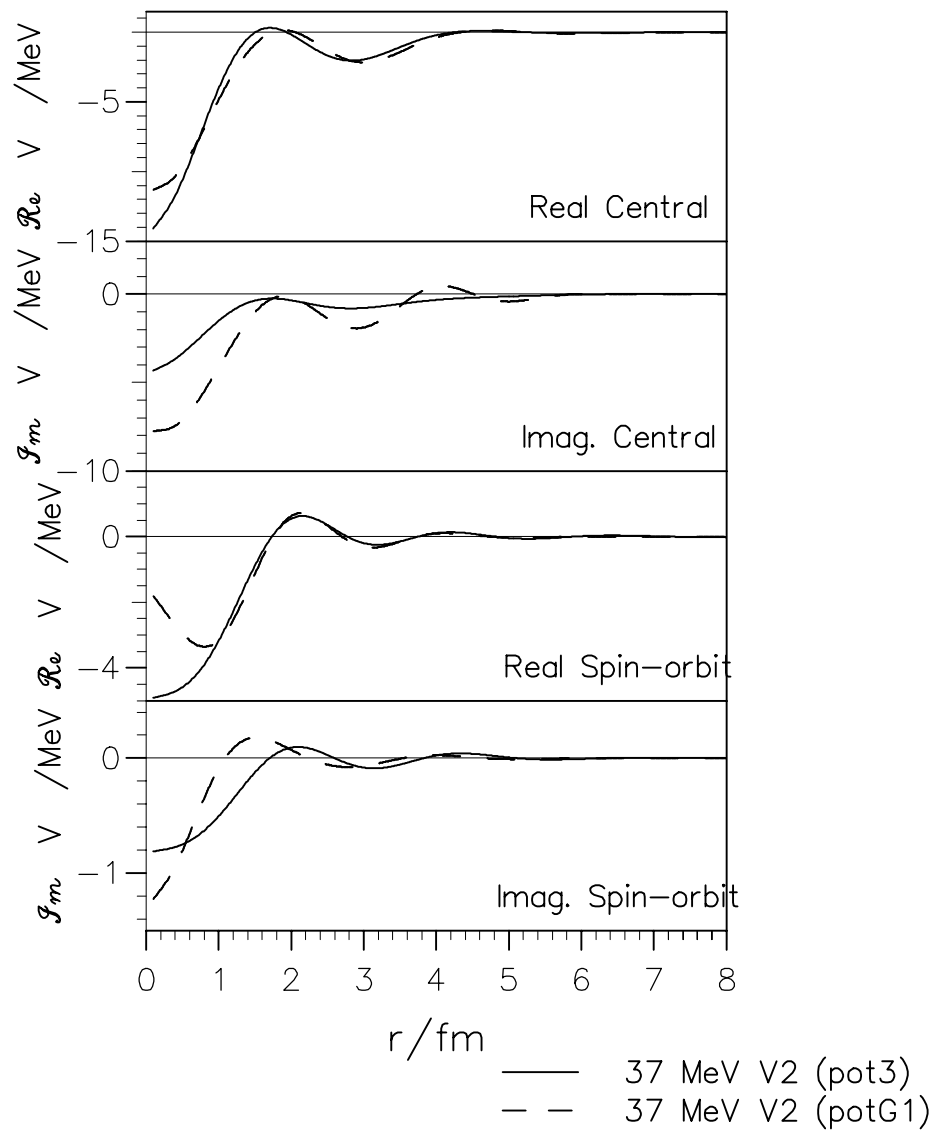
Real Central
Imag. Central
Real Spin–orbit
Imag. Spin–orbit
−5
−15
0
−10
0
−4
0
−1
0 1 2 3 4 5 6 7 8
r/fm
37 MeV V2 (pot3)
37 MeV V2 (potG1)

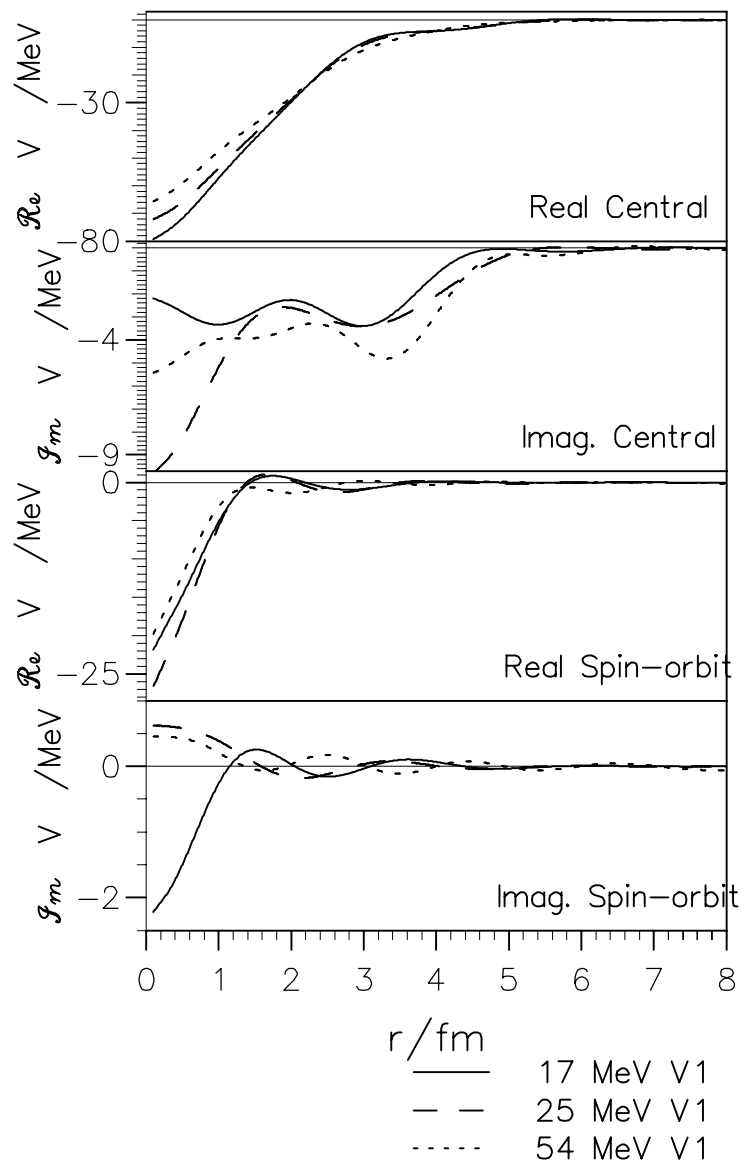
Re V /MeV
−30
−80
Real Central
Im V /MeV
−4
−9
Imag. Central
Re V /MeV
0
−25
Real Spin−orbit
Im V /MeV
0
−2
Imag. Spin−orbit
0 1 2 3 4 5 6 7 8
r/fm
17 MeV V1
25 MeV V1
54 MeV V1

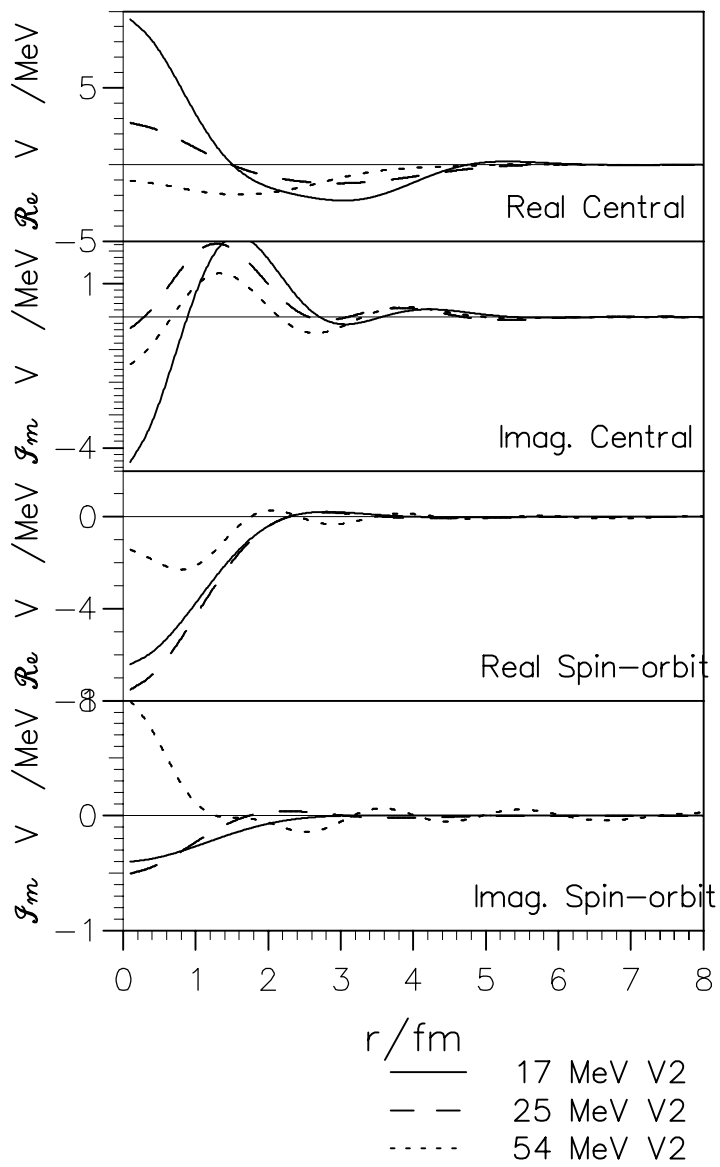
Real Central
Imag. Central
Real Spin−orbit
Imag. Spin−orbit
r/fm
17 MeV V2
25 MeV V2
54 MeV V2